JST: Smart Systems and Devices
Volume 32, Issue 1, January 2022, 059-066

Low-Complexity and Robust Framework of Precoding for Multi-Panel Massive MIMO

Phan Thi Kim Chinh [1], Nguyen Hoai Giang [2], Nguyen Van Son [2], Tran Manh Hoang [3,*]
[1]*Viettel Aerospace Institute, Viettel Group, Hanoi, Vietnam*
[2]*Faculty of Electronics Telecommunication & Information Technology, Hanoi Open University, Hanoi, Vietnam*
[3]*Hanoi University of Science and Technology, Hanoi, Vietnam*
[*]*Email: hoang.tranmanh@hust.edu.vn*

Abstract

Massive multiple-input multiple-output (m-MIMO) is used to improve the robustness of data transmission and high sum spectral efficiency in 5G systems. For 5G New Radio (NR) systems need to be designed to reduce cost and complexity, most notably hybrid analog-digital beamforming with large-scale antenna array which has become a major research target. In the downlink transmission, we propose a robust and low-complexity framework of precoding design to implement hybrid beamforming (BF) of large antenna arrays without limitation on the size of the antenna. Furthermore, a large number of antenna elements can be coupled into multiple panels m-MIMO for the purpose of reducing costs and saving power. This study proposes to use both azimuth and elevation angles parameters to provide low complexity adaptive beam control in panels m-MIMO system. In contrast to existing works, that aim to eliminate inter-user interference, this work is distinguished by adopting polarization function and space-time block code to the m-MIMO antenna arrays. We also propose a new multi-panel codebook design correspondingly with control parameters. The performance of the proposed framework is analysed with state-of-the-art research comparisons. To this end, the important factor of beamforming which is the Error Vector Magnitude (EVM) will be analyzed and simulated.

Keywords: Hybrid beamforming, multi-panel MIMO, 5G, precoding.

1. Introduction

The next generation of wireless networks is expected to truly allow for the interconnection of everything. Additionally, it also has the potential to be transformed into a central and/or distributed sensing, intelligent communications, and computing platform [1]. Furthermore, such networks are also needed to meet the requirements of the connecting of the physical and digital worlds seamlessly and sustainably [2]. However, the conventional approach to fulfill these conditions is either to densify the networks, to turn up the transmit power, or to transmit at a higher frequency band [3]. Nevertheless, due to the scarce of radio frequency associated with the constraint of hardware moving up to a higher frequency seems not to be a feasible solution [4]. Moreover, raising the transmit power and densifying networks will end up in tremendous power consumption. Thus, an alternative solution that not only limits the increase of power consumption but also recycles the current frequency band is desired from both industry and academia [5].

Massive MIMO (m-MIMO) is a key technology for 5G-and-beyond wireless systems by allowing a base station equipped with a very large number of antennas to serve many users at the same time-frequency resource via time-division duplex operation [6]. The first version of 5G new radio (NR) with m-MIMO was standardized by 3GPP. More advanced technologies related to m-MIMO being developed for the future releases of 5G standards. Current m-MIMO systems are deployed based on cellular topology [7]. However, one inherent limitation of cellular-based networks is inter-cell interference, which is mutual interference from other users in other cells to the home cell [8]. Users at the cell boundaries result in bad quality of service because of strong inter-cell interference and path loss, and hence, limit the performance of the whole networks, especially when performing spatial resource allocations [9].

Besides the technique of using multiple phased array antennas, the precoding technique can be considered as a variant of the beamforming technique. In the 5G and beyond wireless communication system, precoding can be conducted in the antenna array (RF) or in baseband (BB) processing, or in both depending on the RF/BB adopted by the transceiver. However, the installation of many antennas in a m-MIMO system leads to difficulties in implementing, hardware, as well as controlling the beams. Recently, the hybrid analog-digital beamforming, which combines beam control by phase shifting at physical antenna ports with precoding matrix to solve such complex problems, has received great attention [11]. To simplify further the connection between research and industry standards, the New

ISSN: 2734-9373
https://doi.org/10.51316/jst.155.ssad.2022.32.1.8
Received: September 14, 2021; accepted: November 2021

Radio (NR) introduces the concept of multi-panel arrays, in which multi-panel arrays are used to form massive antennas. In contrast to existing array architectures, the m-MIMO system using multi-panels will allow each panel or multi-panel to two-stage (analog and digital) steer the beam, providing multiple streams for multiple users. Design wise, the panels can be hung from the ceilings, outside a building, or on a billboard, etc., to increase the coverage gain for 5G signals [12, 13].

In this study, we distinguish it with other works, which is to delve into the research of industry standards for multi-antenna systems using multi-panels. From that, we propose a low-complexity and robust framework of precoding for multi-panel m-MIMO system. Specifically, the traditional precoding matrix will be considered to add azimuth, elevation angle parameters according to 38.214 standardization. With this separation, beamforming can be performed in both the azimuth and elevation domain with two-dimensional antenna array. This spatially separates more users in vertical direction as well as horizontal direction. This is especially important in multi-cell systems, when the users are distributed on the locations defined by the bidirectional axis in each cell. Moreover, the paper evaluates the influence of these two parameters in the extended antenna array models, with multi-panels. We know that multi-panels can expand an unlimited number of antenna arrays, making it cheap to build massive MIMO systems.

On the disadvantage of the massive MIMO systems, where the larger number of antennas is introduced, the dimension of precoding design is getting more complicated. Although the codebooks are also built to simplify the beamforming problem similar to the conventional LTE system, it is nevertheless more difficult to design efficient codebooks. Here, we give a solution to design the precoding matrix for each panel, in a multi-panel antenna array system. In addition, the space-time block coding (STBC) with dual-polarized antenna array is also investigated to provide a good performance of beamforming. In order to underline the validity of our proposed framework, the main beams of the m-MIMO system are described with different azimuth, elevation angle parameters as shown in Fig. 2.

Notation: We use the lower and upper bold letters for vectors and matrices, respectively. $\mathcal{CN}(\cdot,\cdot)$ denotes the circularly symmetric complex Gaussian distribution. $\mathbb{E}\{\cdot\}$ stands for the expectation of a random variable.

2. System Models

This section examines an m-MIMO system, where a BS is equipped with M antennas as most studies usually noted. However, for more detail, we consider this dual-polarized M antennas located in N_g panels. Each panel includes $N_1 \times N_2$ dual-polarized antennas, where N_1 is the number of antennas in the horizontal direction and N_2 denotes the number of antennas in the vertical direction, correspondingly. Thus, we have

$$M = 2 \times N_1 \times N_2 \times N_g. \quad (1)$$

Now we consider this m-MIMO equipped with M antennas, and serves K users, while each user has a single-antenna. In the downlink scenario, the base station (BS) transmits signal vector $\mathbf{x} \in \mathbb{C}^{M\times 1}$, where $\mathbb{E}||\mathbf{x}||^2 = 1$, to all K users. The received signal $\mathbf{y}$ at K users is given as

$$\mathbf{y} = \sqrt{\rho}\mathbf{H}^{\mathbf{T}}\mathbf{x} + \mathbf{n}, \quad (2)$$

where ρ denotes the transmit power weight factor and $\mathbf{n}$ is the additive noise at K users. $\mathbf{H} \in \mathbb{C}^{M\times K}$ represents the channel matrix between the BS and K users. For cellular communication systems in general, the accuracy of the CSI reception is critical to the system's performance. For fast and accurate channel estimation, the codebook mechanism has been used since 3GPP Rel 8.

2.1. Conventional Hybrid Beamforming

Today, hybrid beamforming architectures will take advantage of analog as well as digital beamforming. As shown in Fig. 1, K users are served by the m-MIMO system with hybrid beamforming. The BS is equipped with N_T antennas and N_{RF} RF chains. In this scenario, the phase shifter F_{RF} uses analogy circuitry as in traditional 4G communication systems to form the beam of the signal. However, with the rapid increase in the number of Transceiver Antennas in 5G and Beyond-5G systems, the number of RF chains will become very large.

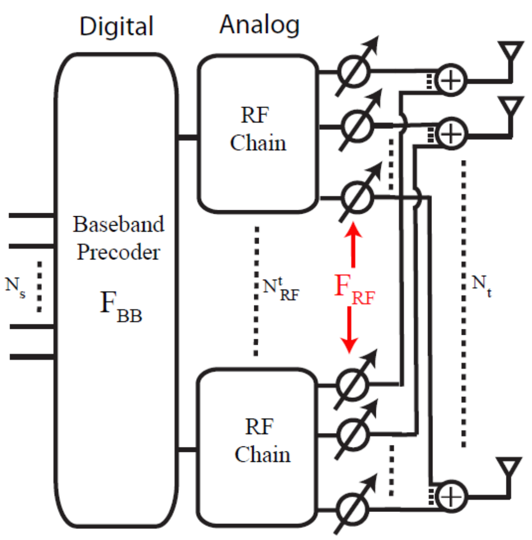

Fig. 1. m-MIMO system with hybrid precoding structure

A fully digital beamforming system requires a separate radio frequency (RF) chain for each antenna. We know that each RF chain is usually quite expensive, with high maintenance costs. n 5G systems and beyond, Ericsson has introduced technology that uses a lot of transmitter antennas. As such, as the number of antennas increases, more RF chains are required. As a result, costs and power consumption are increased. To reduce cost and power consumption, mixed beamforming is constructed by using phase shifters and digital beamforming as shown in Fig. 1. The hybrid beamforming system then uses fewer RF chains than the fully digital beamforming system, and therefore, the system can be built with low hardware complexity.

Furthermore, the codebook-based hybrid beamforming approach is also considered in 5G NR system. This system offers beamforming patterns in accordance with user requirements. Here, the channel states information (CSI) of each user will be stored in the codebook corresponding to the pre-designed precoding. Fig. 2 depicts 16 beamforming patterns of LTE System with Precoding Matrix Selection, correspondingly.

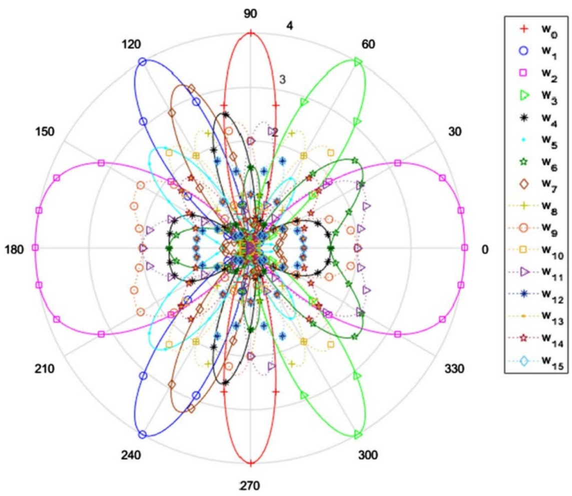

Fig. 2. Beam patterns correspond with Precoding Matrix Selection for LTE System

Leveraging the use of codebooks to simplify beam construction, we introduce two more azimuth and elevation angle factors to control the beam efficiently.

2.2. Precoding Design in Multi-Panel m-MIMO

In multi-panel m-MIMO, we design a low complexity precoding matrix for the purpose of enhancing the performance, rising the spectral efficiency, and minimizing multi-users interference. To enable multi data-stream, N_L layers are precoded in baseband with a precoder $\mathbf{P_{BB}}$. $\mathbf{P_{BB}}$ is the $N_L \times M$ matrix, and the transmit power constraint is ensured by normalizing $\mathbf{P_{BB}}$. This robust architecture enables mapping of N_L data streams to M dual-polarized antennas at $M/2$ physical antenna ports. Let $\mathbf{s}$, is the $N_s \times 1$ transmitted symbol vector, denote the N_L independent data streams, the transmitted signal $\mathbf{x}$ is therefore given as

$$\mathbf{x} = \mathbf{P_{BB}}\mathbf{s}. \tag{3}$$

In short, the received signal is given as

$$y = \sqrt{\rho}\boldsymbol{H}^T\boldsymbol{P}_{\boldsymbol{BB}}\boldsymbol{x} + n. \tag{4}$$

In contrast to other studies, the designed precoding matrix will include azimuth and elevation angle control components. Fig. 3 brings forward an example of a multi-panel antenna structure, where N_g is the number of panels with $N_1 \times N_2$ antenna ports and $2 \times N_1 \times N_2$ polyrod antennas in each panel. a and b stand for the distance between 2 adjacent antenna ports in the same panel and 2 adjacent antenna ports in 2 panels respectively.

In this part, we represent a robust framework that includes four individual functionalities as shown in Fig. 4. More specifically, each task will be demonstrated with corresponding parameters and equations in an effective way.

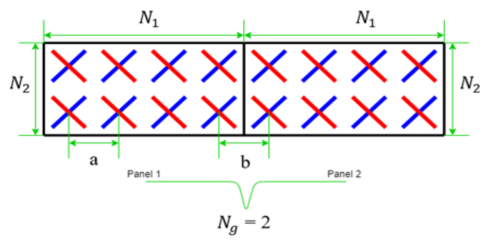

Fig. 3. Multi-panel antenna structure

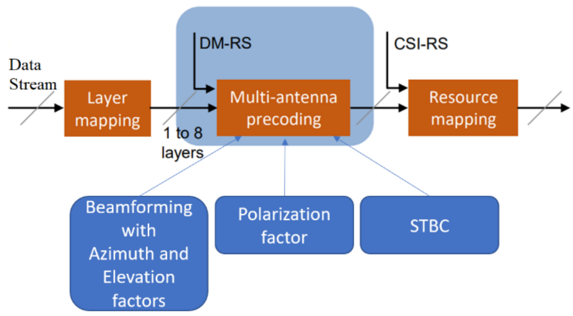

Fig. 4. Robust precoding design with beam management

2.3. Beamforming with Azimuth and Elevation Angle Factors

In order to reduce the computational complexity of precoding design, that helps to form the beam. Let the variables $p \in [0,1,\dots,N_1O_1 - 1]$ and $k \in [0,1,\dots,N_2O_2 - 1]$ determine the sweeping steps of the horizontal and vertical direction, correspondingly. Based on 3GPP standardization 38.214, Rel 15.3-Table 5.2.2.2.2, the supported configurations of (N_g, N_1, N_2) and (O_1, O_2) are given for example in Table 1.

Table 1. Multi-panels massive MIMO configuration.

Number of antenna ports	(N_g, N_1, N_2)	(O_1, O_2)	$N_1 \times O_1$	$N_2 \times O_2$
8	(2,2,1)	(4,1)	$2 \times 4 = 8$	$1 \times 1 = 1$
16	(2,4,1)	(4,1)	$4 \times 4 = 16$	$1 \times 1 = 1$
	(4,2.1)	(4,1)	$2 \times 4 = 8$	$1 \times 1 = 1$
	(2,2,2)	(4,4)	$2 \times 4 = 8$	$2 \times 4 = 8$
32	(2,8,1)	(4,1)	$4 \times 8 = 32$	$1 \times 1 = 1$
	(4,4,1)	(4,1)	$4 \times 4 = 16$	$1 \times 1 = 1$
	(2,4,2)	(4,4)	$4 \times 4 = 16$	$2 \times 4 = 8$
	(4,2,2)	(4,4)	$2 \times 4 = 8$	$2 \times 4 = 8$

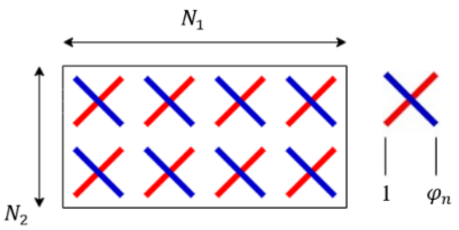

Fig. 5. Logical antenna array with $N_1 = 4$ and $N_2 = 2$, with dual-polarization factor

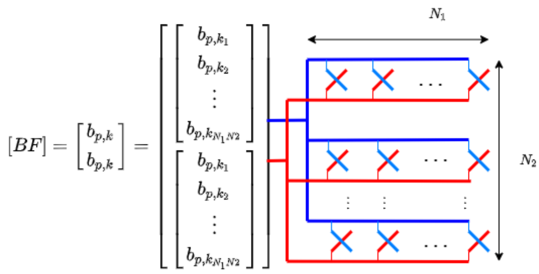

Fig. 6. An illustration of the beamforming matrix that controls each antenna element

To simplify the expressions, let a_p denotes the vertical beam control vector. a_p is given as

$$a_p = \begin{cases} \left[1, e^{\frac{2\pi p}{O_2 N_2}}, \dots, e^{\frac{2\pi p (N_2-1)}{O_2 N_2}}\right] \; for\ N_2 > 1 \\ 1 \; for\ N_2 = 1 \end{cases} \tag{5}$$

Fig. 5 represents the antenna port, with N_1, N_2 are the number of antenna elements in the horizontal and vertical direction. In the actual antenna array, O_1, O_2 are the oversampling factors from logical antenna port to the physical antenna array to rise antenna radiated energy. In short, the number of physical antennas in this case would be $N_1 \times N_2 \times O_1 \times O_2$. In this work, we consider each antenna is dual-polarized with deflection angle φ_n.

This polarization element will be described in the next part, meanwhile, the precoding matrix element $b_{p,k}$ with azimuth p and elevation angle factor k, is designed as

$$b_{p.k} = \left[a_p, a_p e^{\frac{2\pi p}{O_1 N_1}}, \dots, a_p e^{\frac{2\pi p (N_1-1)}{O_1 N_1}}\right]. \tag{6}$$

From (6) it can be seen that, $b_{p,k}$ is designed in baseband domain to manage beamforming in azimuth and elevation angle. $e^{\frac{2\pi k}{O_1 N_1}}$ and $e^{\frac{2\pi p}{O_2 N_2}}$ are the beam control parameters with $k \in (0,1, \dots, O_1 N_1)$and $p \in (0,1, \dots, O_2 N_2)$, that allows adjusting the phase factor vertically and horizontally in the range from 0 degree to 360 degrees. Let [BF] define the beam forming vector in a single panel with 1 layer, it can be interpreted that the [BF] vector comprises $2 \times N_1 \times N_2$ beamforming coefficient as shown in Fig. 6.

2.4. Polarization

To improve energy efficiency, as well as frequency efficiency, the method of using dual-polarization antenna offers additional degrees of freedom to generate beams efficiently. The concept of dual-polarized antenna is based on the angle between two polyrod antenna elements. Different from conventional orthogonal polarization design, we denote the angle $\varphi_n, n \in [1, \dots, 4]$ to design a beam pattern that gives the desired beam shape.

Here, the index n represents four scenarios (vertical, horizontal, right hand or left hand) that control antenna polarization. $n = 0$ means $\varphi_n = 0$ in this case two in phase polyrod antenna creates horizontal polarization.

Similar to the first case, with $n = 1$, $n = 2$ and $n = 3$ we have $\varphi_n = e^{j\pi/2}$, $\varphi_n = e^{j\pi}$ and $\varphi_n = e^{3j\pi/2}$ corresponding with two square-phase polyrod antenna, two reverse phase antenna and two square-phase polyrod antenna creating right (left) hand circular, vertical, and left (right) hand polarization respectively. Therefore, with a specific requirement, it is simple to calculate polarization mask for combining in low complicated precoding matrix.

2.5. Space-Time Block Code

Space-time block code mask has the same size with precoding matrix, separated by space and time between each antenna and between symbols. This function is an essential part, especially in m-MIMO communication. Instead of separating space-time block code in a different step as the conventional model, this paper illustrates the way to integrate it in the precoding matrix. Data after previous masks is encoded utilizing space-time block code, the output is N_L layers

The rows in the space-time block code have orthogonal properties, then ensuring orthogonality in the output signal streams. A space-time block code is defined by a same size with precoding matrix. The number of antenna is used to separate different code from each other.

For instant with space-time block code and input data below illustrate how to separate output

$$\begin{bmatrix} 1 & 1 & 1 \\ 1 & -1 & 1 \\ 1 & 1 & -1 \\ 1 & -1 & -1 \end{bmatrix} \times \begin{bmatrix} X_1 \\ X_2 \\ X_3 \end{bmatrix} \Rightarrow \begin{bmatrix} X_1 + X_2 + X_3 \\ X_1 - X_2 + X_3 \\ X_1 + X_2 - X_3 \\ X_1 - X_2 - X_3 \end{bmatrix}$$

In this example, the 4 outputs $X_1 + X_2 + X_3$, $X_1 - X_2 + X_3$, $X_1 + X_2 - X_3$ and $X_1 - X_2 - X_3$ are independent of each other. Depending on the number of antenna ports and the number of input data streams, the space-time block code mask will be designed accordingly.

Algorithm 1 Solution to precoding matrix.

Input: Channel state information, antenna configuration with N_1, N_2, O_1, O_2, requirement of beam direction, antenna polarization and input data.

1. Consider initial beam direction with range of azimuth and elevation angles, type of polarization and space-time block code. Set up corresponding parameters.
2. **While** have updating requirement for precoding matrix. **do**
    1. Calculate and update parameters p and k with corresponding azimuth and elevation angle given in Table 2.
    2. Consider polarization type and update n.
    3. Specify number of antenna element and input date and compute space-time block code mask.
    4. Calculate energy distribution coefficient.

   End While
3. Multiply precoding matrix with input data.

Output: Data matrix after precoding.

Table 2. Table of precoding parameters description

Parameters	Range Value	Description
k	$0, 1, \ldots,$ $N_1 O_1 - 1$	Vertical Angle control parameter
p	$0, 1, \ldots,$ $N_2 O_2 - 1$	Horizontal Angle control parameter
n	$0, 1, 2, 3$	Polarization control parameter

3. Numerical Results

We consider a massive MIMO system with antenna array configuration N_g = 2, N_1 = 8, N_2 = 2, O_1 = 4 and O_2 = 4 and the number of input layers is $N_L = 2$. The multi-panel MIMO model and system parameters and performance requirements are specified in Table 3.

The antenna polarization cases will be selected with the corresponding requirement. Space-time block code mask with 2 columns and 64 rows with orthogonal property. By using phase array toolbox in Matlab, this paper simulated the way to control beam forming with azimuth and elevation factors. Azimuth angle was controlled by p, we show 2 different cases with the same elevation factor $k = 1$ and show the changes of azimuth angle with increase parameters $p = 1$ and $p = 15$. We can see that azimuth angle was changed with its coefficient as demonstrated in Fig. 8 and Fig. 9. When p increasing from 1 to 15, the number of main beams grows up from 1 to 8 with a larger azimuth angle and diversified directions.

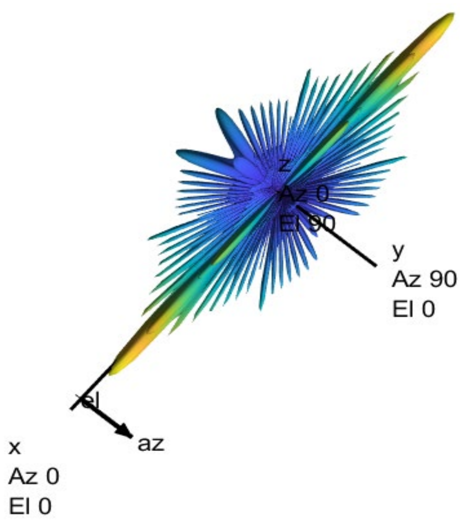

Fig. 8. Control azimuth angle in the first case with parameters $p = 1$ and $k = 1$

Table 3. Multi-panels configuration with N_g, N_1, N_2 parameters

Number of CSI – RS antenna ports	(N_g, N_1, N_2)	CSI Antenna Port Array (Logical Configuration)
8	(2, 2, 1)	
16	(2, 4, 1)	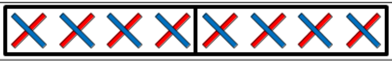
	(4, 2, 1)	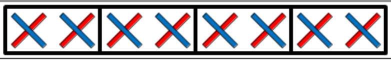
	(2, 2, 2)	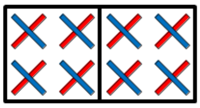
32	(2, 8, 1)	
	(4, 4, 1)	
	(2, 4, 2)	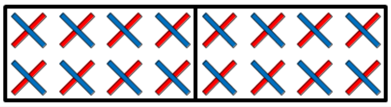
	(4, 2, 2)	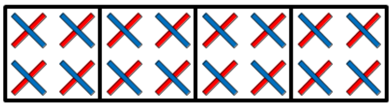

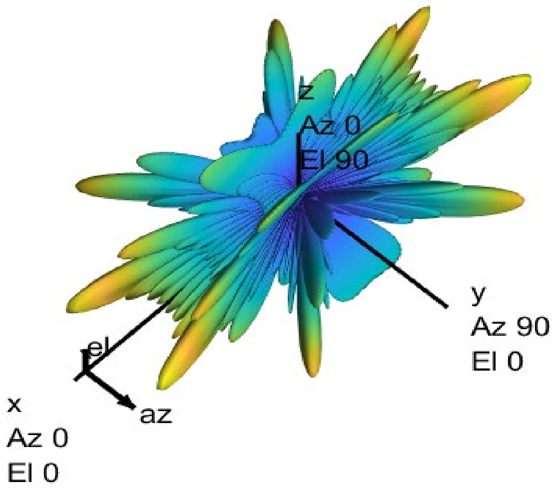

Fig. 9. Control azimuth angle in the first case with parameters $p = 15$ and $k = 1$

When k rises from 1 to 15, the number of main beams increases from 1 to 8 with a larger azimuth angle and diversified directions. In conclusion, depending on different requirements the corresponding azimuth and elevation angle parameters will be calculated.

Similar to the first simulation, Fig. 10 and Fig. 11 proved that the elevation angle control factor will be considered by utilizing the same azimuth factor $p = 1$ and rise elevation angle control parameter with $k = 1$ and $k = 15$. We can see also that more main beams and bigger elevation angles in various directions are created when rising k.

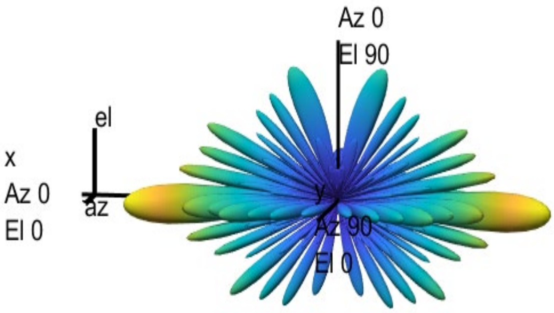

Fig. 10. Control elevation angle in the first case with parameters $p = 1$ and $k = 1$

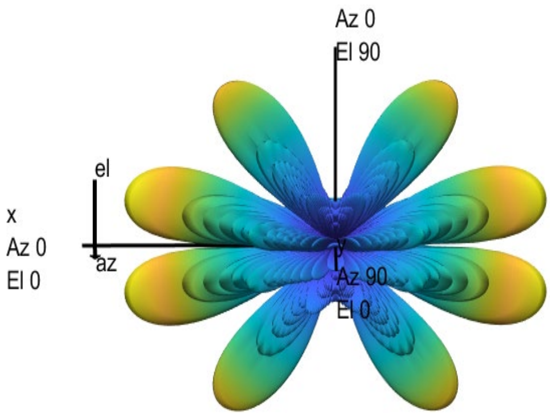

Fig. 11. Control elevation angle in the first case with parameters $p = 1$ and $k = 15$

This paper simulated another example with antenna array configuration $N_g = 4$, $N_1 = 4$, $N_2 = 4$, $O_1 = 4$ and $O_2 = 4$ to indicate how beams change with different antenna configurations. When the number of antenna ports grows up, it means that the radiated energy of the antenna array increases. Fig. 12 shows the simulation result with $p = 1$ and $k = 1$ and the result with $p = 7$ and $k = 7$ is shown in Fig. 13. To compare with the first antenna array configuration simulation, when utilizing the same p, k, more main beams are created due to more radiated energy of the antenna array. In summary, each parameter of four functionalities will be calculated based on specific antenna array configuration and input requirement.

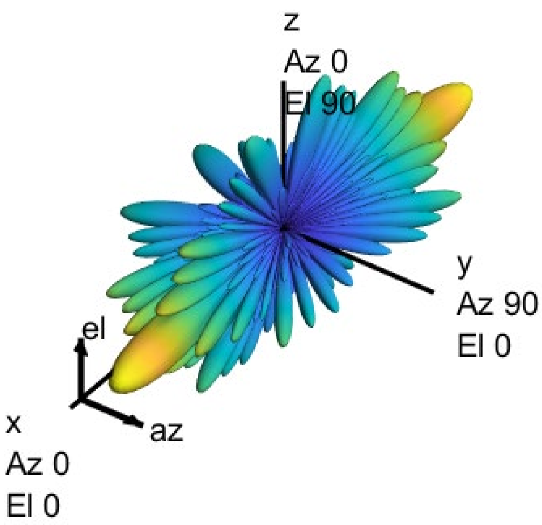

Fig. 12. Beamforming simulation with $p = 1$ and $k = 1$

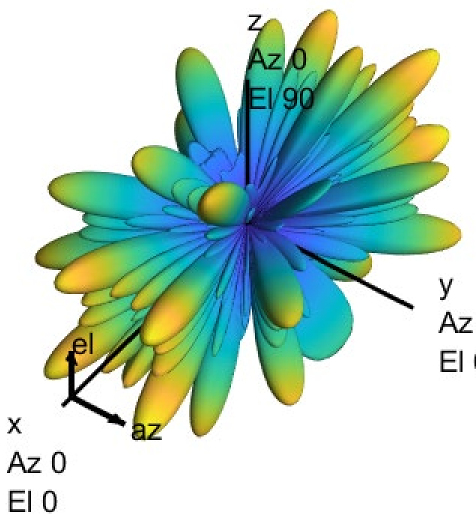

Fig. 13. Beamforming simulation with $p = 7$ and $k = 7$

4. Conclusion

In this paper, we first formalized an overview of low complexity precoding matrix corresponding with the number of antenna ports and input data. Following, a robust framework was proposed to clarify four individual functionalities with specific parameters. Simulation results demonstrate the effectiveness of low computational precoding, beamforming management with azimuth and elevation factors. Future works should progress based on artificial intelligence for real-time processing purposes.

Acknowledgments

This work was funded by Vietnam's Ministry of Education and Training (MOET) Project under Grant B2019-MHN-05.

References

[1] Z. Qin, X. Zhou, L. Zhang, Y. Gao, Y.-C. Liang, and G. Y. Li, 20 years of evolution from cognitive to intelligent communications, IEEE Transactions on Cognitive Communications and Networking, vol. 6, no. 1, pp. 6–20, 2020. https://doi.org/10.1109/TCCN.2019.2949279

[2] K. David and H. Berndt, 6G vision and requirements: is there any need for beyond 5G?, IEEE Vehicular Technology Magazine, vol. 13, no. 3, pp. 72–80, 2018. https://doi.org/10.1109/MVT.2018.2848498

[3] T. H. Nguyen, D. Q. Nguyen, and V. D. Nguyen, Quality of service provisioning for d2d users in heterogeneous networks, EAI Endorsed Transaction on Industrial Networks and Intelligent Systems, vol. 6, p. 160985, 2019. https://doi.org/10.4108/eai.24-10-2019.160985

[4] S. Chen and J. Zhao, The requirements, challenges, and technologies for 5G of terrestrial mobile telecommunication, IEEE Communications Magazine, vol. 52, no. 5, pp. 36–43, 2014. https://doi.org/10.1109/MCOM.2014.6815891

[5] T. H. Nguyen, W.-S. Jung, L. T. Tu, T. V. Chien, D. Yoo, and S. Ro, Performance analysis and optimization of the coverage probability in dual hop LoRa Networks with different fading channels, IEEE Access, vol. 8, pp. 107087–107102, 2020. https://doi.org/10.1109/ACCESS.2020.3000600

[6] T. L. Marzetta, E. G. Larsson, H. Yang, and H. Q. Ngo, Fundamentals of Massive MIMO. Cambridge University Press, 2016. https://doi.org/10.1017/CBO9781316799895

[7] E. Björnson, E. G. Larsson, and M. Debbah, Massive MIMO for maximal spectral efficiency: how many users and pilots should be allocated? IEEE Transactions on Wireless Communications, vol. 15, no. 2, pp. 1293–1308, 2016. https://doi.org/10.1109/TWC.2015.2488634

[8] T. H. Nguyen, T. K. Nguyen, H. D. Han, and V. D. Nguyen, Optimal power control and load balancing for

uplink cell-free multi-user massive MIMO, IEEE Access, vol. 6, pp. 14462–14473, 2018. https://doi.org/10.1109/ACCESS.2018.2797874

[9] H. T. Nguyen, V. C. Trinh, H. Q. Ngo, N. X. Tran, and E. Bjornson, Pilot assignment for joint uplink-downlink spectral efficiency enhancement in massive MIMO systems with spatial correlation, IEEE Transactions on Vehicular Technology, vol. 70, no. 8, pp. 8292-8297, Aug. 2021. https://doi.org/10.1109/TVT.2021.3091020

[10] B. Yang, Z. Yu, J. Lan, R. Zhang, J. Zhou, and W. Hong, Digital beamforming-based massive MIMO transceiver for 5G millimeter-wave communications, IEEE Transactions on Microwave Theory and Techniques, vol. 66, no. 7, pp. 3403–3418, 2018. https://doi.org/10.1109/TMTT.2018.2829702

[11] N. Song, P. Wen, H. Sun, and T. Yang, Multi-Panel based hybrid beamforming for multi-user massive MIMO, in GLOBECOM 2017 - 2017 IEEE Global Communications Conference, 2017, pp. 1–6. https://doi.org/10.1109/GLOCOM.2017.8254880

[12] Y. Huang, Y. Li, H. Ren, J. Lu, and W. Zhang, Multi-Panel MIMO in 5G, IEEE Communications Magazine, vol. 56, no. 3, pp. 56–61, 2018. https://doi.org/10.1109/MCOM.2018.1700832

[13] Le, H. A., Van Chien, T., Nguyen, T. H., Choo, H. & Nguyen, V. D. (2021), 'Machine Learning-Based 5G-and-Beyond Channel Estimation for MIMO-OFDM Communication Systems', Sensors 21(14). https://doi.org/10.3390/s21144861